

X-ray imaging of the solar wind—Mars interaction

Mats Holmström and Stas Barabash

Swedish Institute of Space Physics, Kiruna, Sweden

Esa Kallio

Finnish Meteorological Institute, Geophysical Research, Helsinki, Finland

Abstract. Wherever the solar wind meets a neutral atmosphere, X-rays are emitted by charge-exchange processes between heavy solar wind ions and the neutrals. Using an empirical model of the proton flow near Mars we present computer simulations of X-ray emissions from this charge-exchange process in Mars’ exosphere. We also discuss implications for remote sensing. Here we show that the total X-ray luminosity near Mars from charge-exchange is greater than 10^{25} eV/s for typical solar wind conditions. This flux is large enough to be detected by an X-ray satellite in Earth orbit. Thus, Mars belongs to a new class of X-ray objects in the sky, together with other non-magnetized planets, such as Venus.

Introduction

In 1996 there was a surprising discovery. The Röntgen X-ray Satellite (ROSAT) observed X-ray emissions from comet Hyakutake [Lisse *et al.*, 1996]. Several mechanisms for the emissions were suggested, such as electron bremsstrahlung and scattering of solar X-rays. None of these mechanisms were able to explain the morphology and intensity of the emission region. In 1997 it was suggested [Cravens, 1997] that the X-ray emissions were due to multiply charged heavy solar wind ions excited by charge-exchange with neutral atoms. Computer simulations [Häberli *et al.*, 1997; Wegmann *et al.*, 1998] have shown that this charge-exchange mechanism is consistent with the ROSAT observations. Proof that this is the correct mechanism came recently when NASA’s Chandra X-ray Observatory imaged comet LINEAR and detected X-rays from oxygen and nitrogen ions [Lisse *et al.*, 2000].

X-rays emitted by this charge-exchange mechanism occur wherever the solar wind meets neutral atoms and in this paper we present the results of computer simulations of X-ray emissions near Mars and implications for remote sensing.

Model

Charge-exchange between a multiply charged ion and a neutral atom can leave the ion in an excited state. When the captured electron then transitions to a lower energy state, within L- and K-shells, X-rays may be emitted. This can occur when heavy ions in the solar wind, such as O^{6+} , C^{6+} and Ne^{8+} , interact directly with a planetary neutral atmosphere, e.g., near Mars.

Copyright 2001 by the American Geophysical Union.

Paper number 2000GL000000.
0094-8276/01/2000GL000000\$05.00

We can estimate the radiated power at a point by

$$p = u_{\text{ion}} n_{\text{ion}} n_n \sigma \Delta E \quad [\text{eV}/(\text{cm}^3 \text{ s})], \quad (1)$$

where u_{ion} [cm/s] is the magnitude of the heavy ion velocity, n_{ion} [cm⁻³] is the ion number density, n_n [cm⁻³] is the number density of neutral atoms, σ [cm²] is the cross-section for heavy ion–neutral charge-exchange, and ΔE [eV] is the average emitted energy per heavy ion, that includes the effects of cascading (ions that transition to a lower charge state can transition repeatedly). We regard u_{ion} , n_{ion} and n_n as functions of position, while the rest of the parameters are regarded as constants.

The ion velocities and densities are computed from an empirical, axial symmetric proton flow model based on Automatic Space Plasma Experiment with a Rotating Analyzer (ASPERA) ion measurements on the Phobos-2 spacecraft. The model includes three boundaries: the bow shock (BS), the “magnetopause” (MP, subsolar height = $0.2R_m \approx 680$ km), and the ionopause (IP, subsolar height = $0.05R_m \approx 170$ km). Here R_m denotes Mars’ radii. In the model the proton flux decrease strongly at the MP while the IP represents an impenetrable obstacle for the flow. Charge-exchange collisions are rare near IP because of the low proton flux downstream of the MP (see, Kallio *et al.*, [1997], Fig. 1d and Fig. 7). A detailed model description can be found in Kallio and Koskinen, [1999] and here only certain aspects related to the X-ray emission are considered.

In the empirical model the global electric and magnetic fields can be derived from the velocity model by assuming that the magnetic field is frozen into the flow. The global fields therefore make it possible to study how the ions are accelerated by the Lorentz force near Mars. For example, the solar wind H^+ ion trajectories were found to be described quite well by the flow model for the upstream parameters $u_{\text{sw}} = 400$ km/s and $\mathbf{B}_{\text{sw}} = (0, 2, 0)$ nT in Kallio and Koskinen, [1999].

The role of kinetic effects for the motion of heavy solar wind ions near Mars can be analyzed similarly by studying the motion of ions near the planet. The magnetic field in the empirical flow model, $\mathbf{B}(\mathbf{r})$, is a product of the magnitude of the magnetic field in the solar wind B_{sw} and the normalized magnetic field vector, $\tilde{\mathbf{B}}(\mathbf{r})$, resulting from the frozen-in condition, $\mathbf{B}(\mathbf{r}) = B_{\text{sw}}\tilde{\mathbf{B}}(\mathbf{r})$. The equation of motion for ions relative to the velocity from the empirical model, $\mathbf{U}(\mathbf{r})$, can therefore be expressed as

$$\frac{d^2\mathbf{r}}{dt^2} = (\mathbf{v} - \mathbf{U}(\mathbf{r})) \times \tilde{\mathbf{B}}(\mathbf{r}) \quad [B_{\text{sw}}(m/q)^{-1}], \quad (2)$$

where \mathbf{v} is the velocity of an ion of mass m and electric charge q .

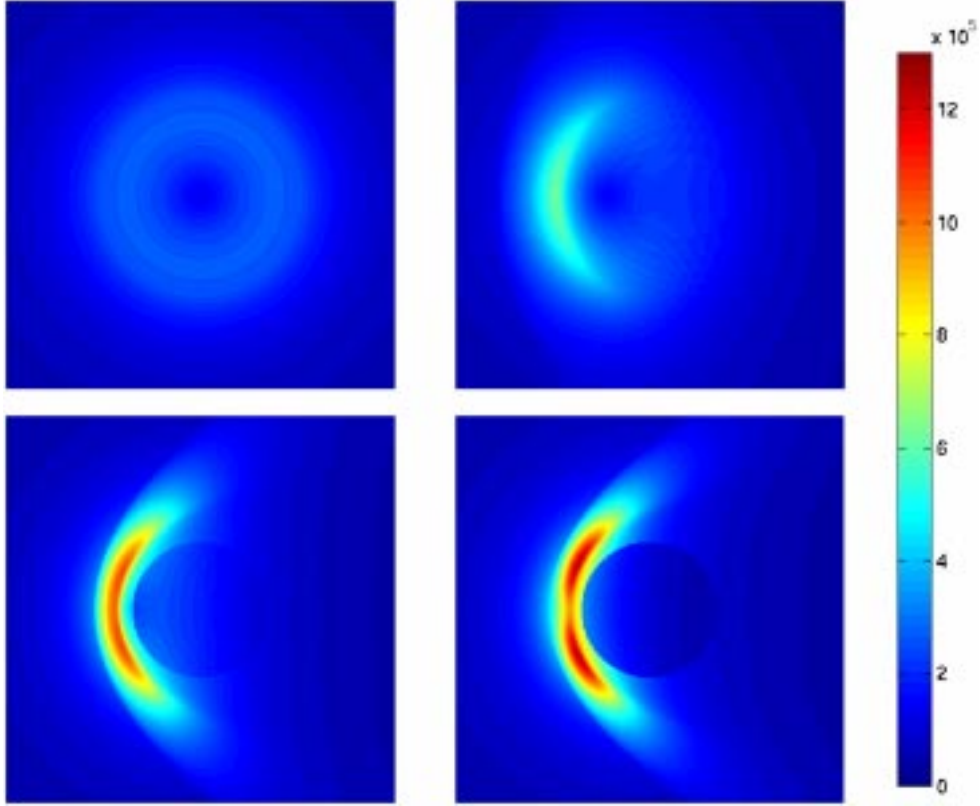


Plate 1. Parallel projections of X-ray emissions near Mars at solar minimum. The angle of the view direction to the Mars—Sun line is, 0 (top left), 30 (top right), 60 (bottom left) and 90 (bottom right) degrees. The intensity is proportional to the directional energy flux [$\text{eV}/(\text{cm}^2 \text{ sterad s})$]. The extent of the images is $6R_m \times 6R_m$, and they are centered at Mars.

Equation (2) illustrates that in the empirical flow model the gyroradius depends linearly on the magnitude of the IMF and the q/m ratio. If two test particles of different q/m values are launched at the same point, at the same initial velocity, their trajectories will be identical for a given solar wind speed if the runs have the same $B_{\text{sw}}(m/q)^{-1}$ value. For example, H^+ ion trajectories presented in *Kallio and Koskinen, [1999]* are identical to the O^{6+} ion ($m/q = 16/6$) trajectories for $\mathbf{B}_{\text{sw}} = (16/6)(0, 2, 0)$ nT = $(0, 5.33, 0)$ nT. About 5 nT magnetic field is therefore strong enough to produce a fluid like motion for the heavy O^{6+} ions.

Diminishing IMF enlarges the ion gyroradius, and thereby increases asymmetric flow features that are not included in the used analytical flow model. Fig. 1 shows an example of the motion of O^{6+} ions calculated for $\mathbf{B}_{\text{sw}} = (0, 4, 0)$ nT. The trajectories suggest that the used flow model give a relatively good approximation for the motion of heavy ions near Mars at typical IMF conditions. The relative number densities of heavy ions in the solar wind can be found in *Wegmann et al. [1998]* and a mean value for m/q of 2.9 can be computed. Justified by the above discussion, we will approximate the heavy ion velocity in (1) by the proton velocity, $u_{\text{ion}} \approx u_p$.

We then approximate the heavy ion number density as a constant fraction, f , of the proton density, $n_{\text{ion}} \approx f n_p$. In practice, as ions charge-exchange along a stream line, the number of ions in highly charged states will decrease. The radiated power then is

$$p = u_p n_p n_n f \sigma \Delta E \quad [\text{eV}/(\text{cm}^3 \text{ s})], \quad (3)$$

where u_p [cm/s] is the magnitude of the proton velocity and n_p [cm^{-3}] is the proton number density.

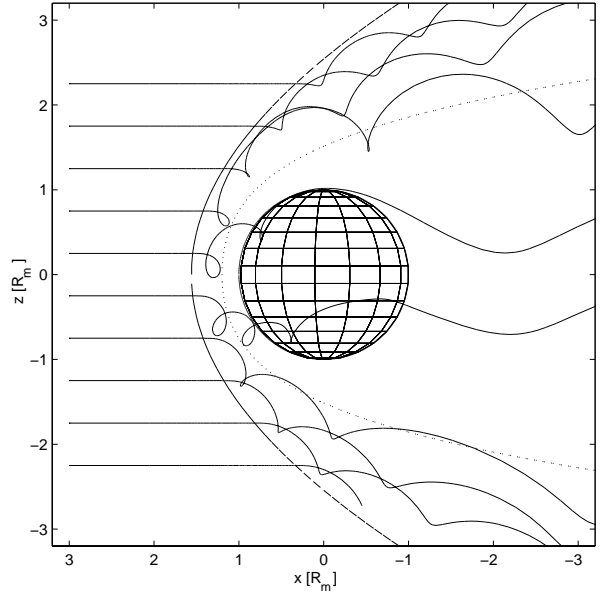


Figure 1. Trajectories for O^{6+} ions ($m/q = 16/6$), when $\mathbf{B}_{\text{sw}} = (0, 4, 0)$ nT and $(u_p)_{\text{sw}} = 400$ km/s. This corresponds to trajectories for H^+ ions when $\mathbf{B}_{\text{sw}} = (6/16)(0, 4, 0)$ nT.

The proton number density, n_p , is computed from the velocity field using mass conservation. The neutral density, n_n , model includes H, H₂ and O, where thermal and non-thermal oxygen are modeled as two separate species. The atomic and molecular hydrogen models are from *Krasnopolsky and Gladstone*, [1996]. The oxygen model is from *Zhang et al.*, [1993]. Each specie's density, n_i , is modeled as

$$n_i(r) = \alpha_i e^{-\beta_i/r} \zeta(\beta_i/r) \quad \text{and} \quad n_n = \sum_i n_i \quad [\text{cm}^{-3}],$$

where r is the distance to the planet's center and ζ is Chamberlain's partition function [Chamberlain and Hunten, 1987]. From *Kallio et al.*, [1997] we have adopted values of the constants α_i and β_i that corresponds to a case of high solar activity (solar maximum) and a case of low solar activity (solar minimum). Due to a lack of data on the exosphere's composition far from Mars, we have limited the computed X-ray emissions to a sphere of radius $10 R_m$ centered at Mars. The error introduced is an under-estimation of the emissions.

Results

We now compute the total luminosity and generate images of the X-ray radiation near Mars using Equation (3). The values of the parameters used in the simulations are those used by *Wegmann et al.* [1998]; $f = 1.08 \cdot 10^{-3}$, $\sigma = 3 \cdot 10^{-15} \text{ cm}^2$ and $\Delta E = 205 \text{ eV}$. Where we have computed $\Delta E = 1137 \text{ eV} \cdot 0.4/2.15$ and $f = 2.15 \cdot 5 \cdot 10^{-4}$ from Wegmann's numbers since their parameters are per oxygen ion and our per heavy ion. For the velocity and density model we have used the solar wind values $(u_p)_{sw} = 400 \text{ km/s}$ and $(n_p)_{sw} = 2.5 \text{ cm}^{-3}$.

Since the X-rays are emitted uniformly in all directions it follows from (3) that the directional emission is $p/(4\pi)$ [eV/(cm³ sterad s)]. To generate images of the radiated X-rays we let the intensity at each pixel in the image be proportional to the total directional emission along the line-of-sight. In Plate 1 we show images from four different vantage points for a neutral model that corresponds to low solar activity.

Note that the proton velocity model is such that the velocity and density are linearly dependent on the solar wind values, $(u_p)_{sw}$ and $(n_p)_{sw}$. Therefore, the emission can increase noticeably, compared to the presented nominal values, when a disturbance of the solar wind hits Mars because the radiated power also depend linearly on $(u_p)_{sw}$ and $(n_p)_{sw}$.

For observations, the emissions directional dependence is of interest. In Fig. 2 we show the maximum directional power emitted by X-rays as a function of the angle between the view direction and the Mars—Sun line for solar minimum and maximum atmospheric models. We see that the directional intensity is between 100 and 1200 keV/(cm² sterad s), depending on solar conditions and view direction. This can be compared with the 11 keV/(cm² sterad s) background of emissions from solar wind charge-exchange with heliospheric H and He estimated by *Cravens* [2000a]. The directional intensity is large enough to be detected (and imaged) by an X-ray satellite in Earth orbit, such as ESA's XMM-Newton X-ray Space Observatory, or NASA's Chandra X-ray Observatory. The expected spectrum of the emissions is that of *Wegmann et al.* [1998] (their Figs. 3 and 4).

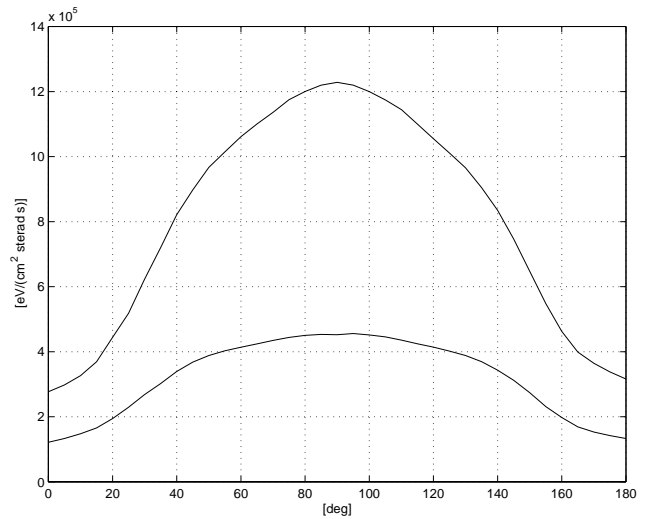


Figure 2. The maximum directional power emitted by X-rays [eV/(cm² sterad s)] as a function of the angle [deg] between the view direction and the Mars—Sun line. The upper graph is for a solar minimum atmospheric model and the lower graph for a solar maximum model.

We also compute the total power emitted by X-rays inside the sphere of $10 R_m$ radius, centered at Mars. At solar minimum this total luminosity is $1.52 \cdot 10^{25} \text{ eV/s}$ and at solar maximum it is $0.93 \cdot 10^{25} \text{ eV/s}$.

Experiments with a non-constant heavy ion fraction, f , along stream lines were performed. This was done by integrating n_{ion} backwards along streamlines to account for ion losses. This resulted in a decrease of the total luminosity by less than 5 %.

We also computed the total X-ray energy flux to Mars' ionopause (subsolar height $0.05 R_m$) as 10^{24} eV/s , or 7 % of the total X-ray production, at solar minimum.

Examining the effect of varying the magnetopause position, it was found that the total luminosity changed by less than 20 % when the subsolar height was varied between 0.1 and $0.5 R_m$. This can be explained by the fact that although the neutral density is high close to the planet, the flow model's proton flux is small.

Comparing our computed total X-ray luminosity of about 10^{25} eV/s to the estimate for Mars of $6 \cdot 10^{22} \text{ eV/s}$ given by *Cravens*, [2000b], our luminosity is almost 170 times larger. We see at least two reasons for this. First of all, *Cravens* estimates the production as $p = 2.5 \cdot 10^{-9} n_n n_p$ [eV/(cm³ s)], with n_p constant. New estimates [*Cravens*, 2000a; *Kharchenko and Dalgarno*, 2000] of the constant ($2.5 \cdot 10^{-9}$) is at least 10 times larger. The constant we have used, from *Wegmann et al.* [1998], is $2.6 \cdot 10^{-8}$. Secondly, *Cravens* only uses hot oxygen as the neutral, but in our model both atomic and molecular hydrogen are included. Using only hot and thermal oxygen in our model, we get a total luminosity of $3 \cdot 10^{23} \text{ eV/s}$, which is consistent with *Cravens'* estimate, taking into account the different production constants.

Implications for remote sensing

There is a fundamental difference between emission of X-rays at Mars and at comets. For comets, due to very large spatial scales of the neutral gas distribution, the heavy ion component of the solar wind is totally depleted while moving

through the cometary coma (that is the reason of the absent of the X-ray emission from the tail) and the peak X-ray flux is determined by the heavy ion density [Dennerl *et al.*, 1997]. In contrast, at Mars, the scale of the neutral gas distribution is small in comparison with the charge-exchange distance and a very small fraction of the solar wind ions is lost during the interaction. This fraction amounts to just a few percent and the loss can be disregarded. That means that comets' X-ray emissions can be used to probe the solar wind while at Mars it is a way to probe the planetary environment.

First of all, X-ray imaging of the near-Mars space opens up an exciting opportunities to remotely diagnose the structure of the solar wind interaction region. If we assume that the neutral gas distribution is known, the deconvolution of X-ray images, for example, via forward-modeling, would provide the global distribution of the solar wind heavy ions. This, in turn, can be converted to the proton distribution. Moreover, it would give extra information about the accuracy of the magnetic field model used in this work because the motion of the heavy ions which could be considered as test particles is governed by the Lorentz force. Since X-ray imaging can be performed in the undisturbed solar wind, simultaneous monitoring of the minor ion density and composition is also possible.

Another interesting application would be to monitor, via X-ray emission, the exospheric (hydrogen) distribution at large distances from the planet where resonance scattering Lyman-alpha emission is too faint to be observed by conventional UV instruments.

All the above considerations are applicable for any other non-magnetized planet/satellite with an atmosphere that is directly exposed to the solar wind. For example, Venus and Titan should emit X-rays according to the same mechanism. Venus looks particularly interesting because the charge-exchange process is more efficient there [Russell *et al.*, 1983].

References

- Chamberlain, J. W., and D. M. Hunten, *Theory of Planetary Atmospheres*, 335 p., Academic, San Diego, Calif., 1987.
- Cravens, T. E., Comet Hyakutake X-ray source: Charge transfer of solar wind heavy ions, *Geophys. Res. Lett.*, *24*, 105-108, 1997.
- Cravens, T. E., Heliospheric X-ray emission associated with charge transfer of the solar wind with interstellar neutrals, *Astrophys. J.*, *532*, L153-L156, 2000a.
- Cravens, T. E., X-ray emission from comets and planets, *Adv. Space Res.*, *26*, 1443-1451, 2000b.

- Dennerl, K., J. Englhauser and J. Trümper, X-ray emissions from comets detected in the Röntgen X-ray satellite all-sky survey, *Science*, *277*, 1625-1630, 1997.
- Häberli, R. M., T. I. Gombosi, D. L. De Zeeuw, M. R. Combi and K. G. Powell, Modeling of cometary X-rays caused by solar wind minor ions, *Science*, *276*, 939-942, 1997.
- Kallio, E., An empirical model of the solar wind flow around Mars, *J. Geophys. Res.*, *101*, 11,133-11,147, 1996.
- Kallio, E., J. G. Luhmann and S. Barabash, Charge exchange near Mars: The solar wind absorption and energetic neutral atom production, *J. Geophys. Res.*, *102*, 22,183-22,197, 1997.
- Kallio, E. and H. Koskinen, A test particle simulation of the motion of oxygen ions and solar wind protons near Mars, *J. Geophys. Res.*, *104*, 557-579, 1999.
- Kharchenko, V. and A. Dalgarno, Spectra of cometary X rays induced by solar wind ions, *J. Geophys. Res.*, *105*, 18,351-18,359, 2000.
- Krasnopolsky, V. A., and G. R. Gladstone, Helium on Mars: EUVE and PHOBOS data and implications for Mars' evolution, *J. Geophys. Res.*, *101*, 15,765-15,772, 1996.
- Lisse, C. M., K. Dennerl, J. Englhauser, M. Harden, F. E. Marshall, M. J. Mumma, R. Petre, J. P. Pye, M. J. Ricketts, J. Schmitt, J. Trümper and R. G. West, Discovery of X-ray and extreme ultraviolet emission from comet C/Hyakutake 1996 B2, *Science*, *274*, 205-209, 1996.
- Lisse, C. M., D. J. Christian, K. Dennerl, F. E. Marshall, R. Mushotzky, R. Petre, S. Snowden, H. A. Weaver, B. Strozozas and S. Wolk, Discovery of charge exchange emission from C/LINEAR 1999 S4, paper presented at DPS Pasadena Meeting, October 23 to 27, 2000.
- Russell, C. T., T. I. Gombosi, M. Horanyi, T. E. Cravens and A. F. Nagy, Charge-exchange in the magnetosheaths of Venus and Mars: A comparison, *Geophys. Res. Lett.*, *10*, 163-164, 1983.
- Wegmann, R., H. U. Schmidt, C. M. Lisse, K. Dennerl and J. Englhauser, X-rays from comets generated by energetic solar wind particles, *Planet. Space Sci.*, *46*, 603-612, 1998.
- Zhang, M. H. G., J. G. Luhmann, S. W. Bougher, and A. F. Nagy, The ancient oxygen exosphere of Mars: Implications for atmosphere evolution, *J. Geophys. Res.*, *98*, 10,915-10,923, 1993.

M. Holmström and S. Barabash, Swedish Institute of Space Physics, PO Box 812, SE-98128 Kiruna, Sweden. (e-mail: matsh@irf.se; stas@irf.se)

E. Kallio, Finnish Meteorological Institute, Geophysical Research, PO Box 503, FIN-00101 Helsinki, Finland. (e-mail: Esa.Kallio@fmi.fi)

(Received September 22, 2000; revised December 12, 2000; accepted December 22, 2000.)